

# Monitoring cathodic protection efficiency and AC induced corrosion using new high-sensitive electrical resistance technology

Lars Vendelbo Nielsen

Department of Manufacturing Engineering, Materials Technology, Technical University of Denmark, building 204, DK-2800 Lyngby, Denmark. [lyn@ipl.dtu.dk](mailto:lyn@ipl.dtu.dk)

## ABSTRACT

A modified differential circuit for ER measurements has been presented which compared with traditional ER principles gives orders of magnitude higher resolution in the electrical resistance measurement. This allows the ER-technique to be applied not only for measurement of degree of accumulated corrosion but also for detection of the instant corrosion rate. The applicability of the modified ER measurement for evaluation of the performance of cathodic protection systems has been demonstrated specifically in the case where AC is superimposed onto the DC protection potential. Unlike other parameters used for assessment of the CP systems infected by AC (maximum peak potential and AC current density), the ER-technique provides data on the instant corrosion rate of the system under investigation. As a special case of AC induced corrosion, it is illustrated by slow DC scans superimposed with AC current as well as by fixed AC/DC conditions for prolonged exposure that superimposed AC is able to induce breakdown of an otherwise stable passive film. This system is under further experimental verification. Besides, the ER-concept is suggested for on-line monitoring tool e.g. as probes connected to pipeline facilities and field test are currently performed.

## KEYWORDS

Pipeline, cathodic protection, coating defect, corrosion rate, ER technique, spread resistance, AC current density, peak potential.

## INTRODUCTION

Evaluation of the efficiency of cathodic protection (CP) systems is usually based on potential measurements. The corrosion rate of the cathodically polarised surface cannot be estimated by traditional electrochemical techniques, since the current flowing under cathodic polarisation is a measure of the cathode activity rather than corrosion. However, electrochemical approaches like *harmonic synthesis* have been suggested [1] involving extrapolation of the anodic Tafel branch in an activation controlled corrosion process to the CP-potential and reading hereby the anodic partial current at that potential.

In the specific case of CP of coating defects in buried pipelines influenced by induced AC current, the CP evaluation becomes complicated, and the usual potential criteria are no longer necessarily valid. Monitoring parameters like AC current density or anodic peak values of the true (IR-free) potential have been suggested [2,3] but these provide no measure of the corrosion rate. Weight-loss coupons connected to the pipeline may be applied but give no indication until removed from the system and brought to the laboratory for examination.

Like in any other corrosion scenario, the ideal corrosion monitoring system should provide a reliable, quick, and simple (“easy-to-interpret”) measurement of the corrosion rate, thereby enabling the CP-operator to take mitigating actions before corrosion develops. This paper suggests a modified electrical resistance (ER) technique to fulfil these demands. The applicability of the technique is demonstrated by examples of corrosion rate measurements obtained under cathodic polarisation and superimposed AC.

## MODIFIED ER TECHNIQUE

ER technology utilises that the electrical resistance of a metal probe element increases when corrosion diminishes the thickness of the element. This technique has several benefits such as simplicity and reliability, and - unlike the electrochemical techniques - there is no demand for a presence of a well-defined electrolyte.

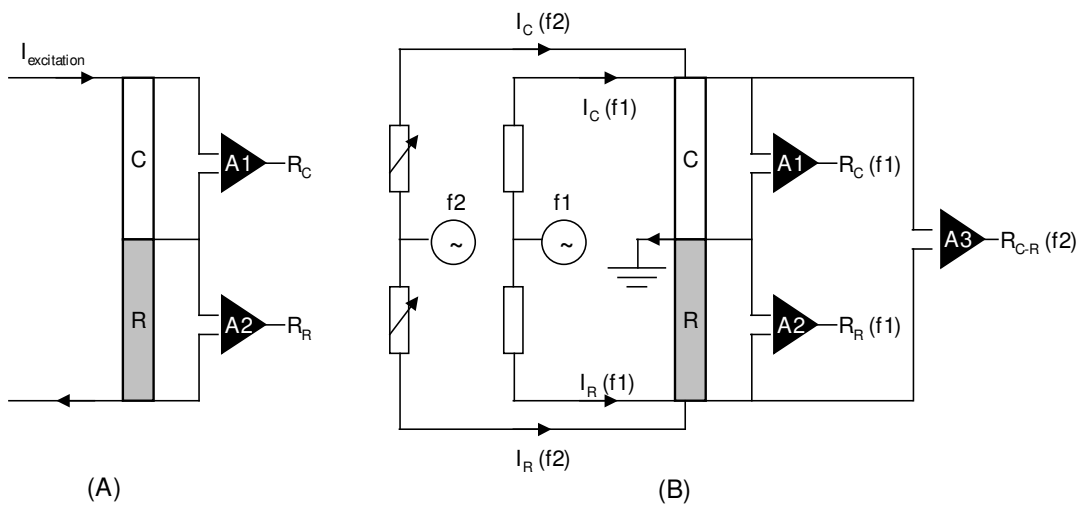


Fig. 1. (A) Traditional ER technology circuit. (B) Modified circuit including differential measurement.

Figure 1(A) shows the principle of the measuring circuit used in traditional ER-techniques. An excitation current is passed through a coupon-element (C) exposed in the corrosive environment and a reference-element (R) shielded from that environment. Amplifiers measure the voltages generated across the elements and convert signals into coupon resistance ( $R_C$ ) and reference resistance ( $R_R$ ). The thickness of the coupon element at time  $t$  ( $\sigma_C(t)$ ) can then (for plate geometry) be assessed by equations like

$$\sigma_C(t) = \sigma_C(t = 0) \cdot \frac{R_C(t = 0)}{R_C(t)} \cdot \frac{R_R(t)}{R_R(t = 0)} \quad (1)$$

The resistance of a reference element is included in the algorithm in order to minimise artefacts caused by temperature changes. The limitation of the technique includes the amount of time needed to produce a measurable increase in resistance of the element, and typically the ER technique can be used solely to assess the degree of accumulated corrosion.

Figure 1(B) shows the modified ER-circuit [4]. Two AC generators provide the excitation currents. AC generator 1 provides current at frequency  $f_1$ . This splits up in two lines, one line feeding the coupon element (C), the other line feeding the reference element (R). The current is returned via grounding in the point between R and C. Phase sensitive and frequency-selective amplifiers A1 and

A2 measure the voltages across C and R and convert these into impedance. The real part impedance can be used to assess degree of accumulated corrosion using equation (1) as in the traditional ER-circuit.

AC generator 2 provides current at frequency f2 different from f1. Again, it splits up in two lines, one line feeding the coupon element (C), the other line feeding the reference element (R). The current is returned via grounding in the point between R and C.

Phase sensitive and frequency-selective differential amplifier A3 measures the voltage difference across C and R and converts this into impedance,  $R_{C-R}$ . Implemented adjustable resistors in the excitation circuit ensure that the differential measurement can be zeroed prior to a corrosion rate measurement, then keeping the dynamic range limited within few milli-ohms. Consequently, the resolution established by suitable amplification is in the order of tenth of a micro-ohm (10-100 times better resolution than traditional ER technology).

Temperature-compensating means can be implemented by making a feed back from the amplifier A2 (measuring voltage across the reference) to the second AC generator (f2) to adjust the level of excitation current so as to keep the reference element voltage constant. This may be implemented as an integrated part of the circuit, by use of microprocessors, or simply by making corrections in a spreadsheet. It can be shown that the temperature coefficient for the differential impedance  $R_{C-R}$  is equal to the temperature coefficient for the material in use.

Since the time change  $dR_{C-R}/dt$  of the real part of the differential impedance is a measure of the time change in resistance of the coupon element, the corrosion rate  $V_{corr}$  can be calculated using the equation:

$$V_{corr} = \frac{dR_{C-R}}{dt} \cdot \frac{W}{L} \cdot \frac{\sigma^2}{\rho} = \frac{dR_{C-R}}{dt} \cdot \frac{\rho}{R^2} \cdot \frac{L}{W} \quad (2)$$

where L is length of element, W is width of element,  $\sigma$  is element thickness, and  $\rho$  is (temperature dependent) material resistivity. Equation (2) can be rearranged to predict necessary measuring time  $\Delta t$  as a function of the corrosion rate, the element dimensions, and the instrument resolution  $\Delta R$ :

$$\Delta t = \frac{\Delta R}{V_{corr}} \cdot \frac{W}{L} \cdot \frac{\sigma^2}{\rho} \quad (3)$$

It is observed that the factor  $L/(W\rho^2)$  relating to the element dimensions is a measure of the probe sensitivity. A high-sensitive probe can be manufactured by increasing length to width ratio or by decreasing the element thickness [5]. The latter implies that the probe lifetime decreases as well. The modified differential measurement benefits from high probe sensitivity as well, but additionally, in relation to equation (3), the modified differential ER measurement enhances resolution of the measurement by orders of magnitude.

## EXPERIMENTAL

The experiments were performed using variants of the circuit diagram sketched in figure 2. A traditional three-electrode electrochemical cell was used in which an ER-probe acted as working electrode. The ER-probes used here were very simple disposable electrodes prepared from 25- $\mu$ m thin iron foil mounted on a printed circuit board. The reference part of the element was shielded

from the environment by epoxy coating. Electrode area was 2 cm<sup>2</sup>. The probe was continuously connected to the ER instrumentation and signals R<sub>C</sub>, R<sub>R</sub>, and R<sub>C-R</sub> picked up by a datalogger.

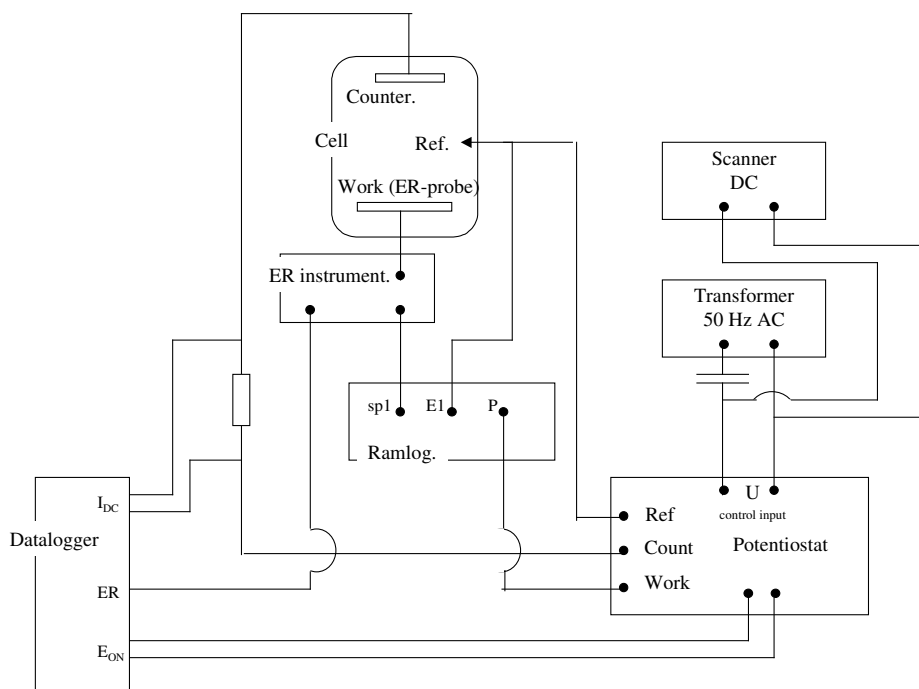


Fig. 2. Diagram of the set up used for AC corrosion studies.

The electrical signals were imposed via a potentiostat system. A Ramlog Correal recorder (the functionality of which as presented by Pourbaix et al [3]) was inserted in the working electrode circuit in order to pick up IR free potentials by the build-in automatic current interruption technique. The recorder picked up instant current values as well.

Examples of corrosion measurements in three different solutions are presented here. The solution chemistry is outlined in table 1.

Component	Solution (concentration in mol/L)		
	1	2	3
MgSO <sub>4</sub> .7H <sub>2</sub> O	0.0025	-	-
CaSO <sub>4</sub> .2H <sub>2</sub> O	0.0025	-	-
NaHCO <sub>3</sub>	0.0025	0.0025	0.1
CaCl <sub>2</sub>	0.0050	-	-
Na <sub>2</sub> SO <sub>4</sub>	-	0.005	-
NaCl	-	0.01	-
Na <sub>3</sub> PO <sub>4</sub>	-	-	0.1
pH	7.80	8.20	9.15
Conductivity (μS/cm)	1900	2530	11120

Table 1. Chemical composition of test solutions.

The constituents of solution 1 included earth alkaline cations (Mg<sup>2+</sup> and Ca<sup>2+</sup>) which in combination with hydroxyl ions generated by the CP produce resistive layers at the surface thereby increasing

the spread resistance (ohmic resistance) of the system. Results are shown from a condition of  $-850$  mV DC polarisation superimposed by  $2.12$  V AC (provided by a coupled AC generator, figure 2) fixed for about 70 hours.

Solution 2 was produced as close as possible to solution 1 with regard to concentration of the anions, however the earth alkaline cations in solution 1 were replaced by the alkaline cation  $\text{Na}^+$  in order to prevent formation of resistive layers. In this series of experiments, the ER probe was first subjected to a pure DC by running a slow polarisation scan ( $30$  mV/hour using a coupled DC scanner, figure 2) from  $-1150$  mV SCE to  $-550$  mV SCE (ON-potential). This was subsequently repeated with a superimposed  $100$  A/m<sup>2</sup> 50 Hz AC current.

Solution 3 was a pH 9.15 passivating  $\text{NaHCO}_3/\text{Na}_3\text{PO}_4$  buffer that has been pointed out earlier by Pourbaix et al [3] to show some unpleasant behaviour towards steel when AC is involved. Results from DC scans with superimposed 50 Hz ( $300$  A/m<sup>2</sup>) AC is presented. The scans were run from the passive open circuit potential (around  $-300$  mV CSE) to  $-1100$  mV SCE then reversed. Further, the results from fixed conditions ( $-850$  mV SCE with  $300/400$  A/m<sup>2</sup> AC) are shown.

## RESULTS AND DISCUSSION

Figure 3 shows the results from the 70-h experiment in solution 1. Figure 3(A) illustrates the potential oscillation caused by the AC current. It seems to be rather stable in between  $-800$  and  $-900$  mV SCE in the first half of the experiment and displaces slightly in the anodic direction thereafter. Figure 3(B) illustrates the results from the differential ER-measurement and the corrosion rate accordingly calculated from equation (2).

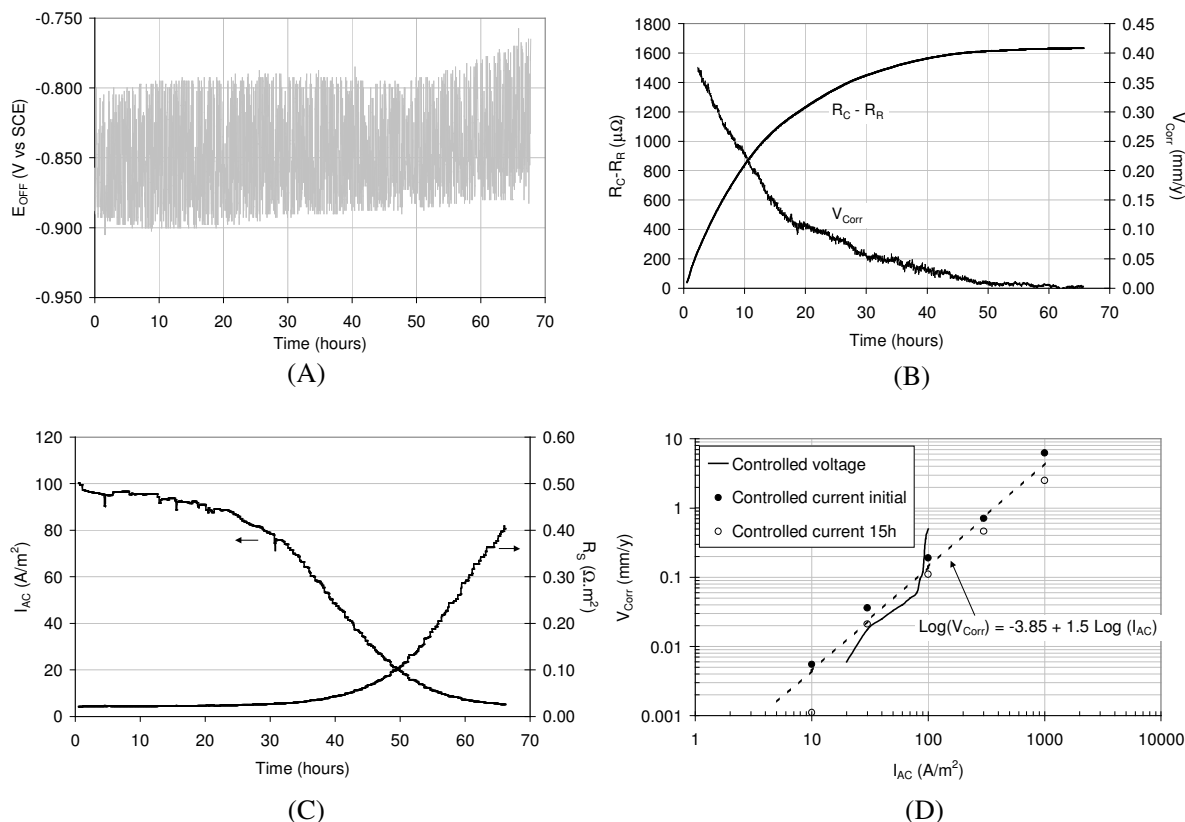


Fig. 3. Results obtained in solution 1 – fixed AC/DC condition throughout a 70-h period.

As observed, the corrosion rate decays over time even though the maximum anodic peak potential displaces in the anodic direction at the same time. This illustrates merely that although the anodic peak potential may be one applicable parameter for monitoring AC corrosion, it tells just as little about corrosion rate as does the electrochemical potential measured in a common pure DC situation.

Figure 3(C) illustrates the AC current density and the ohmic spread resistance  $R_s$  throughout time. The AC current density is regulated by the constant AC voltage (2.12 V) divided by the spread resistance of the system. As observed, the AC current density decays over time as the spread resistance increases due to formation of resistive products at the electrode surface.

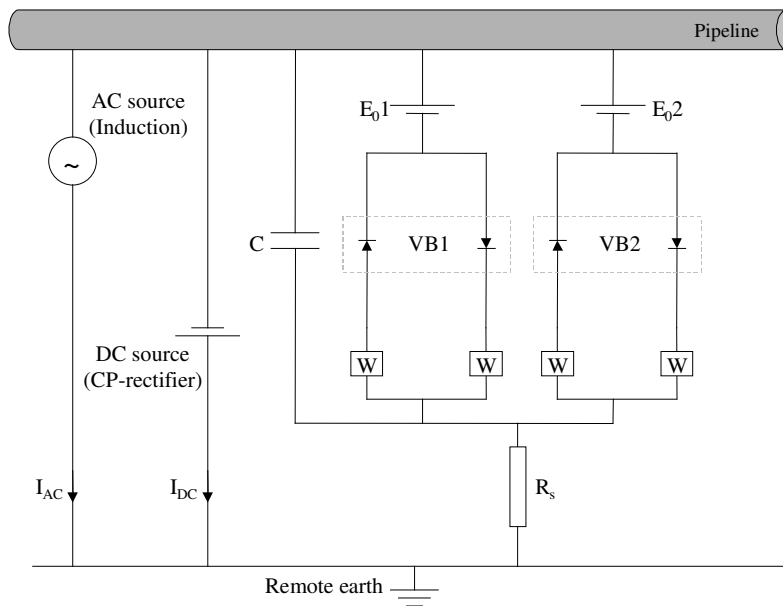


Fig. 4. Electrical equivalent circuit proposed to aid in interpretation of AC corrosion [6].

Figure 4 illustrates an electrical equivalent circuit that has been proposed previously [6] to apply to AC corrosion problems. A DC source in the form of a CP rectifier provides the cathodic protection to the pipeline coating defects by imposing a DC voltage in between the pipe and remote earth. In parallel herewith, an AC source is positioned to account for induced AC voltage. The 50 Hz AC current flowing in between a coating defect and remote earth is passed via the ohmic spread resistance  $R_s$  and to a great extent shorted by the capacitance  $C$  of the interface. Activation controlled electrochemical processes are represented as Volmer-Butler “diodes” in series with Warburg impedances accounting for effects of “long-term” ( $\gg 20$  ms) diffusion processes. Two electrochemical electrode processes are included in the figure, which could be iron dissolution ( $\text{Fe} \rightarrow \text{Fe}^{2+} + 2e$ ) and the reverse ( $\text{Fe}^{2+} + 2e \rightarrow \text{Fe}$ ) as the VB1 process and a cathode process like hydrogen ion reduction or oxygen reduction as the second VB2 process. In relation to the correlation between AC current density and the spread resistance of the system, this correlation shows that the 50 Hz impedance of the interfacial capacitor is very minor to the polarisation resistance of the processes described through the individual Volmer-Butler equations.

In figure 3(D) is illustrated by the continuous line the measured corrosion rate versus the AC current density. This line shows that when the increasing spread resistance decreases the AC current density, the corrosion rate decreases as well. In the same figure is included experimental results from the same system in which the AC current density was kept constant for a 15-h period rather than the AC voltage (reported elsewhere [7]). It appears from the illustrated behaviour that in this system the corrosion rate may be a function of the AC current density. However, since initial corrosion rates are significantly higher than the corrosion rates measured after 15 hours in the

controlled current experiments, one would interpret this as an increase in the polarisation resistance relating to the corrosion process. In other words, the electrochemical characteristics of the processes do change over time – just like it is often observed in DC corrosion (polarisation or depolarisation). The observed behaviour may be sustained from the fact that an ever-decreasing AC current density does not result in an ever-decreasing magnitude of the potential oscillation (figure 3(A)).

Figure 5 shows the results from the scan performed in solution 2. The scans were performed in this solution rather than the scale forming solution 1 in order to exclude effects of increased spread resistance throughout the scan period.

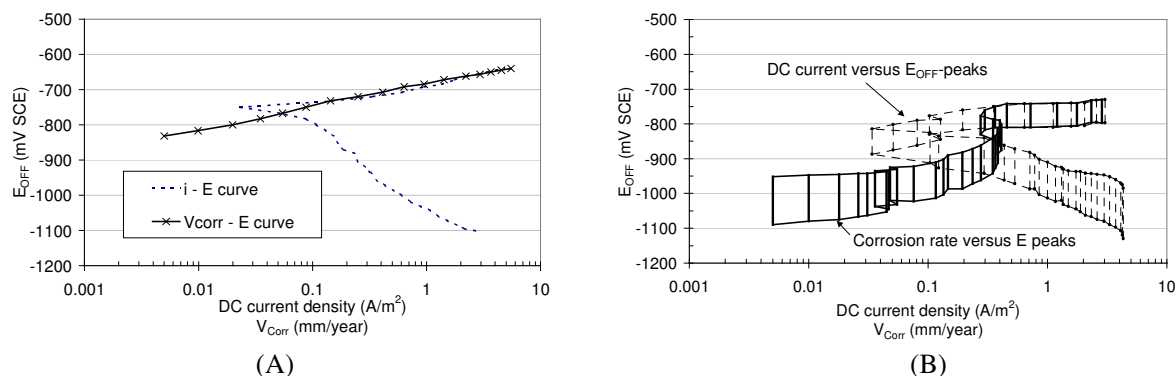


Fig. 5. Results from scans performed in solution 2.

Figure 5(A) shows the DC scan in which the current density in the activated anodic branch should correlate perfect with corrosion rate of the metal. The corrosion rate measured with the ER technique confirms this correlation. The point being here that under cathodic polarisation of the metal, the corresponding current is of cause no measure of corrosion, but apparently, the corrosion rate measured with the ER-technique provides a very plausible curve also under the cathodic polarisation. Figure 5(B) shows the similar curves obtained with superimposed AC (100  $A/m^2$ ). The polarisation curves are now showing a degree of potential oscillation. From the corrosion rates measured with and without AC it is observed that the AC provides quite an activation effect on the iron dissolution reaction – at least during these short-term polarisation experiments. In the AC case, the corrosion rates do not seem to be consistent with any extrapolation of the anodic branch.

Figure 6 shows results obtained in solution 3. In addition to the results shown, a DC scan was performed, and there was no detectable corrosion occurring in the entire potential range. Figure 6(A) is the cathodic scan with superimposed AC current (300  $A/m^2$ ). As observed, the corrosion increases as the potential becomes more negative and a peak in corrosion rate occurs in the region  $-800$  to  $-100$  mV SCE after which the corrosion rate decays again. Figure 6(B) is the reversed (anodic) scan in which a peak in corrosion rate (this time with a higher corrosion rate) is observed again. These curves clearly show that the superimposed AC is able to destabilise a passive film, which is otherwise formed when only DC is imposed onto the electrode.

Figure 6 (C) shows the results from fixed AC/DC condition ( $-850$  mV SCE DC and 300/400  $A/m^2$  AC). These results show that the corrosion decays over time but seems to approach a steady state corrosion rate. A similar experiment performed with  $-300$  mV (SCE) DC offset potential superimposed by 300  $A/m^2$  AC showed no sign of corrosion. As also indicated by Pourbaix et al [3], the influence of the AC seems to be that the passive film reduces during the negative half cycle, whereas the formation of passive iron oxides is too slow to keep up with the 50 Hz AC during the positive half cycle.

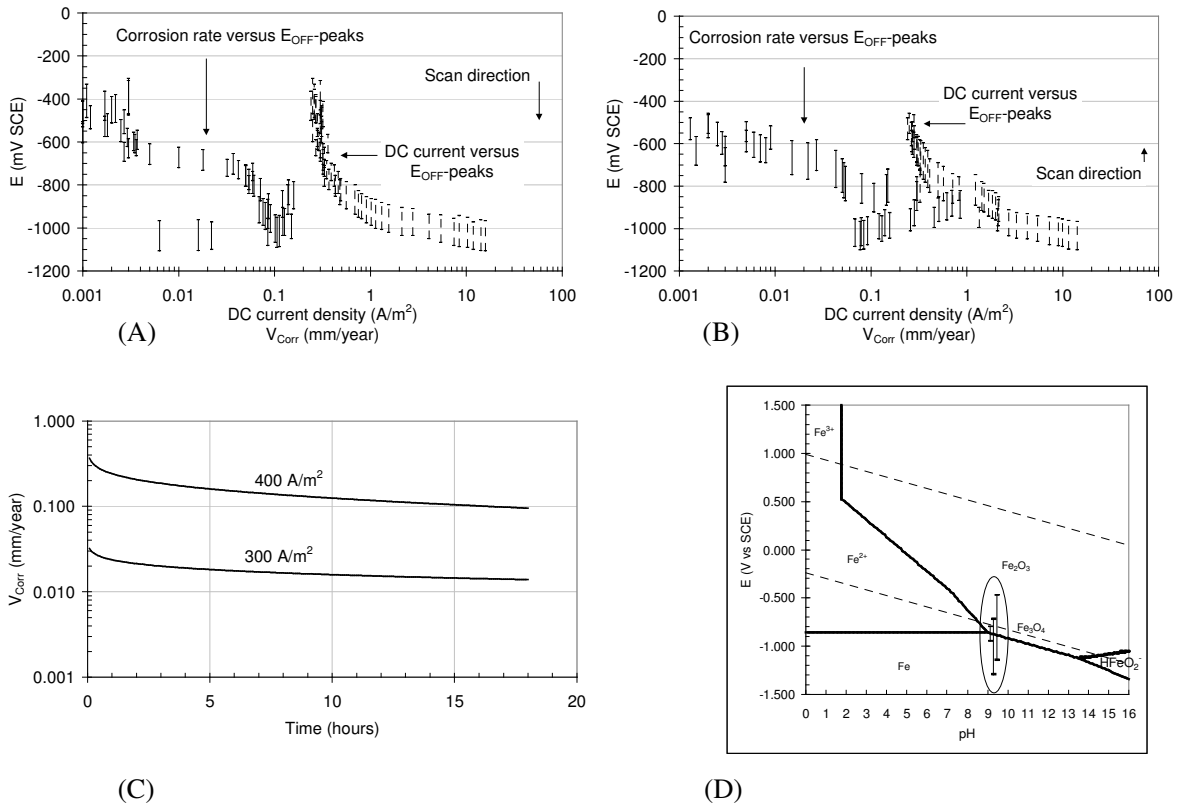


Fig. 6. Results obtained in solution 3.

No	$E_{ON}$ mV SCE	$E_{OFF}$ (max) mV SCE	$E_{OFF}$ (min) mV SCE	$I_{AC}$ $A/m^2$	$V_{corr}$ mm/year
1	-300	-300	-475	300	0
2	-850	-800	-950	300	0.040 / 0.014
3	-850	-725	-1300	400	0.400 / 0.095
4	-700	-470	-1150	686	2.080

Table 2. Corrosion rate observations under fixed AC/DC conditions in solution 3. Corrosion rate given in number 2 and 3 reflects initial and final value. Number 4 is data given by Pourbaix et al [3].

Table 2 outlines the results obtained in fixed AC/DC experiment in solution 3. Number 4 is data presented by Pourbaix et al [3] who investigated the exact same system, however at different AC/DC load ( $E_{DC} = -700$  mV,  $I_{AC} = 686$   $A/m^2$ ). They found a very high corrosion rate under these circumstances. The tendency from the table seems quite clear. The simultaneous condition of a cathodic peak potential favouring reduction of the passive film and an anodic peak potential ranging far into the otherwise passive region prohibits the formation of the passive film and the steel corrodes. The peak potentials outlined in table 2 have been inserted into the Pourbaix diagram (figure 6(D)) for illustration.

## CONCLUSIONS

A modified differential circuit for ER measurements has been presented which compared with traditional ER principles gives orders of magnitude higher resolution in the electrical resistance measurement. This allows the ER-technique to be applied not only for measurement of degree of accumulated corrosion but also for detection of the instant corrosion rate. The applicability of the modified ER measurement for evaluation of the performance of cathodic protection systems has been demonstrated specifically in the case where AC is superimposed onto the DC protection potential. Unlike other parameters used for assessment of the CP systems infected by AC (maximum peak potential and AC current density), the ER-technique provides data on the instant corrosion rate of the system under investigation. As a special case of AC induced corrosion, it is illustrated by slow DC scans superimposed with AC current as well as by fixed AC/DC conditions for prolonged exposure that superimposed AC is able to induce breakdown of an otherwise stable passive film. This system is under further experimental verification. Besides, the ER-concept is suggested for on-line monitoring tool e.g. as probes connected to pipeline facilities and field test are currently performed.

## ACKNOWLEDGEMENTS

- Studies on AC corrosion sponsored by DONG Natural Gas A/S.
- ER-technology developed and sponsored by VN-Instrument I/S.

## REFERENCES

1. J. Jankowski, Evaluation of cathodic protection performance by harmonic synthesis, Proc. EUROCORR 2000, London (2000), Institute of Materials (2000), topic 16.
2. F. Stalder et al. AC corrosion on cathodically protected pipelines, Proc. 5<sup>th</sup> international congress CeoCor, Brussels (2000).
3. Pourbaix et al, Measurement of the importance of AC induced corrosion, Proc. EUROCORR 2000, London (2000), Institute of Materials (2000), topic 16.
4. International patent application, PCT/DK00/00689, Method and apparatus for measuring accumulated and instant rate of material loss or material gain, VN-Instrument (2000).
5. Ridd et al, Field trials using a new generation of electrical resistance probe for the optimisation of chemical corrosion inhibitors, Proc. EUROCORR'97, Trondheim (1997), Vol. 1 p. 189.
6. L.V. Nielsen, P. Cohn, AC corrosion and electrical equivalent diagrams, Proc. 5<sup>th</sup> international congress CeoCor, Brussels (2000).
7. L.V. Nielsen, AC corrosion rates of cathodically polarised steel exposed in a scaling, neutral pH soil solution, Technical report, Dept. of manufacturing engineering. (2001).
8. L.V. Nielsen, AC corrosion rates of steel exposed in non-scaling soil solution – correlation with DC scans. Technical report, Dept. of manufacturing engineering. (2001).